Journal of Inorganic Biochemistry 204 (2020) 110963

Contents lists available at ScienceDirect

Journal of Inorganic Biochemistry

journal homepage: www.elsevier.com/locate/jinorgbio

Synthesis, characterization and albumin binding capabilities of quinizarin containing ternary cobalt(III) complexes

Máté Kozsup[a], Orsolya Dömötör[b], Sándor Nagy[a], Etelka Farkas[a], Éva A. Enyedy[b], Péter Buglyó[a,*]

[a] Department of Inorganic and Analytical Chemistry, University of Debrecen, Egyetem tér 1, H-4032 Debrecen, Hungary
[b] Department of Inorganic and Analytical Chemistry, Interdisciplinary Excellence Centre, University of Szeged, Dóm tér 7, H-6720 Szeged, Hungary

A B S T R A C T

Four Co(III) ternary complexes with the composition of $[(Co(4\ N))_2(quin)](ClO_4)_4$ or $[(Co(4\ N))_2(quinS)](ClO_4)_3$, where 4 N = tris(2-aminoethyl)amine (tren) or tris (2-pyridylmethyl)amine (tpa), $quinH_2$ = quinizarin (1,4-dihydroxy-9,10-anthraquinone), $quinSH_3$ = quinizarin-2-sulfonic acid (1,4-dihydroxy-9,10-anthraquinone-2-sulfonic acid), were synthesized, characterized and their human serum albumin (HSA) binding capabilities were also tested. The complexes can be considered as likely chaperons of quinizarins which are structural models for anthracycline-based anticancer drugs like doxorubicin. All the Co(III) complexes are dinuclear and were isolated as mixture of isomers. Comparison of the cyclic voltammograms of the free ligands and the appropriate Co(III) complexes revealed that the new signals belonging to reversible processes in the range −400–0 mV (vs. Ag/AgCl) for the complexes can be attributed to the reversible reduction of the Co(III) centre. These potentials are in the range of typical (O,O) chelated Co(III) ternary complexes bearing 4 N donor ligands and follow the order being more positive for the tpa containing complexes. Presence of the sulfonate group in the quinizarin results in slightly more negative reduction potential of the Co(III) complexes. HSA binding capabilities of the $quinH_2$ and $quinSH_3$ ligands as well as the appropriate complexes showed that $quinSH_3$ has higher affinity to the protein than $quinH_2$ while none of the complexes seem to bind to HSA.

1. Introduction

Drawbacks associated with the lack of selectivity of square planar Pt (II) complexes currently used in the treatment of some tumors may be eliminated by taking into consideration the differences of healthy and tumor cells. For this purpose, inert Co(III) complexes for instance may serve as promising candidates since with suitable donor atom environment these compounds can undergo selective reduction in the more reductive environment of the cancer cells caused by hypoxia. As a consequence, ligands with anticancer potential can be released upon dissociation of the less stable Co(II) complex within the cancer cell.

Anthracyclines are a class of antineoplastic drugs derived from *Streptomyces* sp. First anthracyclines were isolated from *Streptomyces peucetius* and were named doxorubicin and daunorubicin. These quinizarin (1,4-dihydroxy-9,10-anthraquinone, $quinH_2$) based molecules with anticancer activity play an important role in the treatment of breast, ovarian, lung cancer, a range of neuroblastomas and leukemia [1–4]. The cellular target of doxorubicin is topoisomerase II enzyme. By interfering with the topoisomerase II-DNA complex doxorubicin inhibits the enzyme thus triggers cell death because of the formation of double-strand breaks of DNA by the direct intercalation with DNA duplex. This event inhibits the DNA replication and transcription to mRNA [1,5–8]. Doxorubicin and other anthracycline drugs suffer from dose-dependent acute and chronic toxicity the latter being due to cardiotoxicity. The cardiotoxicity of doxorubicin is connected to iron-mediated various electron transfer processes resulting in the formation of reactive oxygen species (ROS) and subsequent generation of oxidative phosphorylation and lipoperoxidation [9–18]. Recently it was also reported that doxorubicin-induced cardiotoxicity is mediated by topoisomerase-IIβ in heart muscle cells [8]. Anthracyclines with O-donors in chelate forming position are good metal ion complexing agents. A large number of literature data indicate that endogenous iron plays an important role in the dose-dependent cardiotoxicity of the anthracycline drugs. Iron is believed to be involved in ROS formation and the redox cycling of quinone form of doxorubicin would enable to increase the cellular levels of iron by mobilizing of iron from ferritin resulting in higher level of oxidative stress. On contrary to the “ROS hypothesis” it was also demonstrated that on the one hand iron chelators like dexrazoxane are capable of decreasing the doxorubicin-related cardiotoxicity, on the other hand none of the tested antioxidants proved to be protective against chronic cardiotoxicity in clinical settings [4,19–21].

Beside iron the complexation of anthracyclines with some other metal ions were also studied. In earlier works Garnier-Suillerot et al. have studied the complex formation between Fe(III) or Pd(II) and doxorubicin, daunorubicin or carminomycin. It was found that all these anthracyclines form stable tris complexes with the Fe(III) while with Pd (II) bis and dimeric (Pd:ligand = 2:2) complexes were assumed. Despite the high stability of the Fe(III) complexes, complex dissociation

* Corresponding author.
E-mail address: buglyo@science.unideb.hu (P. Buglyó).

https://doi.org/10.1016/j.jinorgbio.2019.110963
Received 8 October 2019; Received in revised form 11 December 2019; Accepted 15 December 2019
Available online 17 December 2019
0162-0134/

followed by intercalation of the unbound ligand into the DNA base pairs was observed in in vitro studies. Furthermore, all these complexes displayed anticancer activity against P-388 leukemia cells [22–24]. The complexation of doxorubicin with Cu(II) and Fe(II) was also investigated and found that [CuL_2] or [FeL_3] are the major species at pH = 7.0 [25]. In a more recent study the interaction of doxorubicin and its structural model, 1,4-dihydroxy-9,10-anthraquinone-2-sulfonate (quinizarine-2-sulfonic acid, quinSH_3), with Ni(II) was studied. The bis-ligand complexes, found to be present in solution, are able to bind to calf thymus DNA. Notably, the drug complex was reported to have much higher stability than the other model complex [26].

Regarding the simpler structural model of the anthracyclines, quinizarin, its dinuclear Ru(III) and Os(II) complexes in which the quinizarin acts as a bridging ligand were synthesized and characterized. In both cases the redox study of the complexes revealed the non-innocent behaviour of the anthraquinone and several oxidation and reduction steps of the complexes were detected [27,28].

The aim of this work was to synthesize and characterize novel mixed ligand Co(III) complexes bearing the quinH_2 ligand or its sulfonate derivative quinSH_3 as models for the costlier anthracycline drugs, in order to explore the nuclearity, stability, kinetic and redox behaviour of the complexes. In these species four coordination sites of the central Co (III) is taken by tripodal tetramines in order to provide appropriate redox features [29,30]. Tris(2-aminoethyl)amine (tren) and tris(2-pyridylmethyl)amine (tpa) tripodal amines were selected for the studies. According to our hypothesis these Co(III) mixed ligand species may undergo selective dissociation under hypoxic conditions releasing the bioligand mostly in tumor cells. In an ideal case if the ligand is released selectively in the tumor cells it can be assumed that the dose of the anthracycline drug administered in metal complexed form can be lowered, and the dose-dependent cardiotoxicity of the anthracyclines can be minimized. Herein we present the synthesis, characterization and human serum albumin (HSA) binding results of four novel Co(III) ternary complexes with the model quinH_2 or quinSH_3 ligands accessed by elemental analysis, NMR and infrared (IR) spectroscopy, electrospray ionization mass spectrometry (ESI-MS), cyclic voltammetry (CV), UV–visible (UV–Vis) and fluorimetric methods. The formulae of the used ligands and the complexes are summarized in Fig. 1.

2. Experimental

2.1. Materials and reagents

$CoCl_2 \cdot 6H_2O$, $NaNO_2$, tren, $NaClO_4$, NH_4PF_6, 1,4-dihydroxy-9,10-anthraquinone (quinH_2), 1,4-dihydroxy-9,10-anthraquinone-2-sulfonic acid (quinSH_3), D_2O, d^6-DMSO were commercial products from Merck, Sigma-Aldrich, Reanal, Pflatz and Bauer. Tpa [31], [Co(tren)$(NO_2)_2$]Cl, [Co(tren)Cl_2]Cl, [Co(tpa)$(NO_2)_2$]Cl, [Co(tpa)Cl_2]Cl [32] were synthesized and purified according to literature procedures. HSA (with fatty acids as lyophilized powder), warfarin (WF), dansylglycine (DG), *n*-octanol and all buffer components (KCl, NaCl, $Na_2HPO_4 \cdot 2H_2O$, KH_2PO_4) were Sigma-Aldrich products in *puriss* quality. Milli-Q ultrapure water was used as solvent for the samples and stock solutions. CAUTION: Although we never have experienced any problems, perchlorate salts are potentially explosive.

2.2. Synthesis of the complexes

2.2.1. [(Co(tren))$_2$(quin)](ClO$_4$)$_4$ (1)

QuinH_2 (38 mg, 0.16 mmol) was dissolved in 10 mL isopropanol containing 2 eq. 1M KOH (320 μL), giving a purple solution. [Co(tren)Cl_2]Cl (100 mg, 0.32 mmol), dissolved in 5 mL water, was added. The brown/deep orange mixture was heated at reflux for 4 h. The mixture was kept at room temperature overnight. The solid was filtered off and $NaClO_4$ was added to the solution in excess. Purple crystalline solid appeared after a few hours, on standing at 4 °C. The crude product was washed with 2 mL MeOH and recrystallized from acetonitrile. The solid was filtered off and dried in vacuo. Yield: 72 mg (43%). ^{1}H NMR (400 MHz, D_2O): δ/ppm = 8.46 (m, 2H, Ar—H); 7.94 (m, 2H, Ar—H); 7.46 (t, 1H, Ar—H); 7.37 (t, 1H, Ar—H); 3.94 (m, 2H, -CH_2); 3.84 (m, 2H, -CH_2); 3.54 (m, 4H, -CH_2); 3.37 (m, 4H, -CH_2); 3.24 (m, 4H, –CH_2); 3.07 (m, 6H, –CH_2); 2.88 (m, 2H, –CH_2). (400 MHz, d^6-DMSO): δ/ppm = 8.44 (m, 2H, Ar—H); 7.96 (m, 2H, Ar—H); 7.47 (t, 1H, Ar—H); 7.28 (t, 1H, Ar—H); 5.48 (m, 4H, -NH_2); 5.32 (m, 4H, -NH_2); 5.24 (m, 3H, -NH_2); 5.13 (m, 1H, -NH_2); 3.58 (m, 4H, -CH_2); 3.41 (m, 4H, -CH_2); 3.21 (m, 4H, -CH_2); 3.00 (m, 4H, -CH_2); 2.85 (m, 4H, -CH_2); 2.78 (m, 4H, -CH_2). IR (KBr)/cm^{-1}: 3260, 1543, 1422, 1105, 625. Anal. Required for $C_{26}H_{42}Cl_4Co_2N_8O_{20} \cdot 0.8NaClO_4 \cdot 0.6\ H_2O$: C, 27.03, H, 3.77,

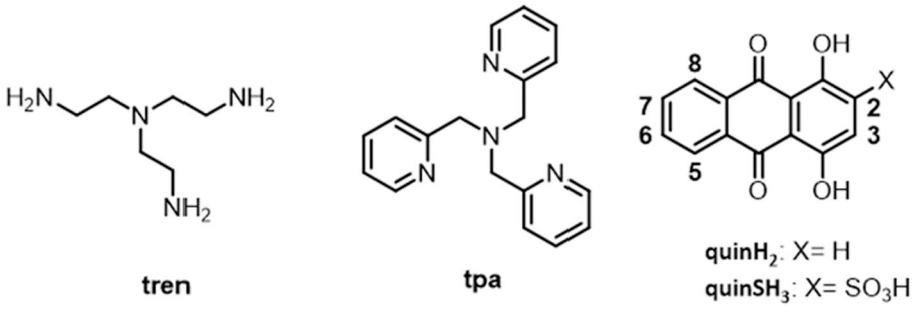

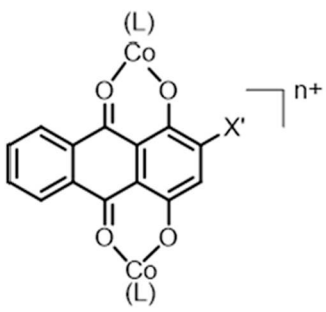

	L	X'	n
1	tren	H	4
2	tpa	H	4
3	tren	SO_3^-	3
4	tpa	SO_3^-	3

Fig. 1. Structure and abbreviation of the studied ligands and complexes.

N, 9.70%. Found: C, 27.00, H, 3.78, N, 9.58%. MS (ESI, positive ion): *m/z*: 444.122 ([Co(II)(tren)(quin) + H]$^+$); 304.037 ([Co(II)(tren)(ClO_4)]$^+$).

2.2.2. [(Co(tpa))$_2$(quin)](ClO_4)$_4$ (2)

The synthesis was similar to that of **1**, using [Co(tpa)Cl_2]Cl (100 mg, 0.22 mmol), quinH_2 (26 mg, 0.11 mmol), 1 M KOH (220 μL). The crude product was washed with 2 mL MeOH and Et_2O and it was recrystallized from water. The complex was isolated as an indigo coloured crystalline solid. Yield: 94 mg (47%). ^{1}H NMR (400 MHz, d^6-DMSO): *δ*/ppm = 9.44 (d, 0.5H, Ar−H); 9.37 (m, 1.5H, Ar−H); 9.11 (d, 0.5H, Ar−H); 8.59 (d, 0.5H, Ar−H); 8.46 (m, 0.5H, Ar−H); 8.32 (m, 1.5H, Ar−H); 8.24 (m, 3H, Ar−H); 8.12 (m, 8H, Ar−H); 7.85 (m, 8H, ArH); 7.57 (m, 1H, ArH); 7.41 (m, 5H, ArH); 5.86 (m, 2.5H, -CH_2); 5.70 (m, 1.5H, -CH_2); 5.35–5.17 (m, 6H, -CH_2); 5.06–4.96 (m, 2H, -CH_2). IR (KBr)/cm^{-1}: 3434, 3083, 1611, 1540, 1424, 1278, 1091, 770, 623. Anal. Required for $C_{50}H_{42}Cl_4Co_2N_8O_{20}$·2 H_2O: C, 43.81, H, 3.38, N, 8.18%. Found: C, 43.95, H, 3.34, N, 8.26%. MS (ESI, positive ion): *m/z*: 588.119 ([Co(II)(tpa)(quin) + H]$^+$); 468.099 ([(Co(II)(tpa))$_2$(quin)]$^{2+}$); 448.034 ([Co(II)(tpa)(ClO_4)]$^+$); 174.542 ([Co(II)(tpa)]$^{2+}$).

2.2.3. [(Co(tren))$_2$(quinS)](PF_6)$_3$ (3)

QuinSH_3 (51 mg, 0.16 mmol) was dissolved in 10 mL MeOH and 2 eq. 1M KOH (320 μL), was added giving a purple solution. [Co(tren)Cl_2]Cl (100 mg, 0.32 mmol), was added and the mixture was stirred at 60 °C for overnight. The mixture was filtered after standing at 4 °C for half a day. Purple solid appeared immidiately by adding NH_4PF_6 (78 mg, 0.48 mmol). The mixture was heated at reflux to get a clear solution and left to cool down to room temperature slowly. Purple crystalline solid appeared. The solid was filtered off and dried in vacuo. Yield: 78 mg (48%). ^{1}H NMR (400 MHz, d^6-DMSO): *δ*/ppm = 8.41 (m, 2H, Ar−H quinS); 7.93 (m, 2H, Ar−H quinS); 7.75 (s, 0.5H, Ar−H quinS); 7.60 (s, 0.5H, Ar−H quinS); 6.02 (m, 1H, -NH_2); 5.90–5.67 (m, 7H, -NH_2); 5.45 (m, 2H, -NH_2); 5.25 (m, 1H, -NH_2); 5.06 (m, 1H, -NH_2); 4.26 (m, 2H, -CH_2); 3.57 (m, 2H, -CH_2); 3.42 (m, 2H, -CH_2); 3.25–3.11 (m, 4H, -CH_2); 2.98 (m, 5H, -CH_2); 2.85 (m, 7H, -CH_2); 2.63 (m, 2H, -CH_2). IR (KBr)/cm^{-1}: 1602, 1413, 1048, 639, 501, 419. Anal. Required for $C_{26}H_{41}Co_2F_{18}N_8O_7P_3S$: C, 26.86, H, 3.55, N, 9.64, S, 2.76%. Found: C, 26.51, H, 3.46, N, 9.95, S, 2.58%. MS (ESI, positive ion): 363.070 ([(Co(III)(tren))$_2$(quinS)-H]$^{2+}$); 304.035 ([Co(II)(tren)(ClO_4)]$^+$).

2.2.4. [(Co(tpa))$_2$(quinS)](ClO_4)$_3$ (4)

QuinSH_3 (51 mg, 0.16 mmol) was dissolved in 10 mL water and 2 eq. 1M KOH (320 μL), was added giving a purple solution. [Co(tpa)Cl_2]Cl (146 mg, 0.32 mmol) dissolved in 5 mL water was added and the mixture was stirred at 70 °C for 4 h. 20 mL propanol and $NaClO_4$ in excess were added. On standing at 4 °C purple crystalline solid appeared. The solid was filtered and dried in vacuo. Yield: 132 mg (63%). ^{1}H NMR (400 MHz, d^6-DMSO): *δ*/ppm = 10.31 (d, 1H, Ar−H tpa); 9.44 (d, 1H, Ar−H tpa); 8.83 (s, 1H, Ar−H quinS); 8.45 (d, 2H, Ar−H tpa); 8.41 (d, 2H, Ar−H); 8.34 (m, 2H, Ar−H); 8.11–7.98 (m, 6H, Ar−H); 7.84 (m, 3H, Ar−H); 7.77 (t, 4H, Ar−H); 7.69 (t, 1H, Ar−H); 7.62 (t, 2H, Ar−H); 7.56 (t, 2H, Ar−H); 7,40 (dd, 2H, Ar−H); 5.73 (dd, 4H, -CH_2); 5.33 (d, 4H, -CH_2); 5.19 (dd, 4H, -CH_2). IR (KBr)/cm^{-1}: 1612, 1450, 1050, 637, 504, 419. Anal. Required for $C_{50}H_{41}Cl_3Co_2N_8O_{19}S$·0.5 propanol·2 H_2O: C, 44.81, H, 3.58, N, 8.12, S, 2.32%. Found: C, 44.82, H, 3.57, N, 7.95, S, 2.53%. MS (ESI, positive ion): 667.068 ([Co(III)(tpa)(quinS) + H]$^+$); 507.573 ([(Co(III)(tpa))(quinS)(Co(II)(tpa))]$^{2+}$); 174.543 ([Co(II)(tpa)]$^{2+}$).

2.3. NMR, IR and ESI-MS measurements

NMR measurements were carried out using Bruker Avance 400 NMR spectrometer at room temperature on samples prepared in D_2O or/and in d^6-DMSO. Calibration was performed using the signals of the solvents (2.50 ppm for DMSO and 4.79 ppm for D_2O). IR spectra as KBr pellets were recorded on a Perkin Elmer FTIR Paragon 1000 PC instrument at the Department of Organic Chemistry, University of Debrecen. ESI-TOF MS measurements in the positive mode were carried out on a Bruker micrOTOF-Q instrument at the Department of Applied Chemistry, University of Debrecen. The concentration of the samples was 10 μg/mL and the solvent was water or methanol. The instrument was equipped with an electrospray ion source, where the voltage was 4 kV. The drying gas was N_2. The flow rate was 4 L/min and the drying temperature was 200 °C. The spectra were recorded by means of a digitizer at a sampling rate of 2 GHz. The mass spectra were calibrated externally, using the exact masses of clusters [(NaTFA)$_n$ + Na]$^+$ generated from the electrosprayed solution of sodium-trifluoroacetate (NaTFA). The spectrums were evaluated with DataAnalysis 3.4 software from Bruker. The samples were introduced directly into the ESI with a syringe pump at a flow rate of 3 μL/min.

2.4. Cyclic voltammetric (CV) studies

Cyclic voltammetric experiments were performed within the voltage range 0 – −1000 mV, at room temperature in H_2O or MeOH, using a Metrohm 746–747 VA Trace Analyser and BASi Epsilon EClipse equipped with a three-electrode system, which consists of a Ag/AgCl/3 M KNO_3 reference electrode ($E_{1/2}$ = +209 mV vs. normal hydrogen electrode (NHE)), a platinum wire auxiliary electrode (ALS Co. Japan), and a glassy carbon (CHI104) working electrode. Aqueous solution of $K_3[Fe(CN)_6]$ was used to calibrate the system ($E_{1/2}$ = +0.458 V versus NHE in 0.50 M KCl) [33]. The samples were degassed before the measurements using argon gas. The concentration of the complexes was 1 mM, the potential sweep rates were 200 mVs^{-1} during the determination of the redox potentials. The supporting electrolyte contentration was 0.20 M in all cases. KNO_3 was used in aqueous solutions and [NBu_4][BF_4] was used in methanolic solutions. Ligands quinH_2 and quinSH_3 were dissolved in water by adding one drop of base (0.2 M KOH). The samples were dissolved in methanol for pH dependence studies and pH was adjusted by 0.2 M HCl and 0.2 M KOH.

2.5. Lipophilicity measurements

Distribution coefficients ($D_{7.40}$) of the compounds were determined by the traditional shake-flask method in *n*-octanol/buffered aqueous solution at pH = 7.40 phosphate buffer saline (PBS) at 25.0 ± 0.2 °C. Compounds, except for quinH_2, were dissolved in *n*-octanol pre-saturated buffered aqueous phase, and final compound concentration was 20–100 μM. Ligand quinH_2 was dissolved in *n*-octanol pre-saturated by water in 2 mM concentration. Aqueous buffered phases and water pre-saturated *n*-octanolic phases were gently mixed in 1:1, 1:70 (for **3**, **4**), or 20:1 (for quinH_2) volume ratios with Heidolph Reax 2 overhead shaker (~20 rpm) for 2 h. The mixtures were centrifuged with Eppendorf MiniSpin Plus centrifuge (5000 rpm, 3 min). After phase separation, UV − Vis spectrum of the compound in the aqueous phase (in the *n*-octanolic phase in case of quinH_2) was compared to that of the original stock solution and D_{pH} values of the compounds were calculated according to the following equations:

$$D_{pH} = \left[\frac{Abs_{(stock.sol.)}}{Abs_{(aqueous\ phase\ after\ separation)}} - 1\right] \times \frac{V_{(aqueous\ phase)}}{V_{(n-octanol\ phase)}} \quad (1)$$

and for quinH_2:

$$D_{pH} = \left[\frac{Abs_{(oct.phase\ after\ separation)}}{Abs_{(stock.sol.)} - Abs_{(oct.phase\ after\ separation)}}\right] \times \frac{V_{(aqueous\ phase)}}{V_{(n-octanol\ phase)}} \quad (2)$$

A Hewlett Packard 8452a diode array spectrophotometer was used to measure the UV–Vis spectra in the interval 200–500 nm.

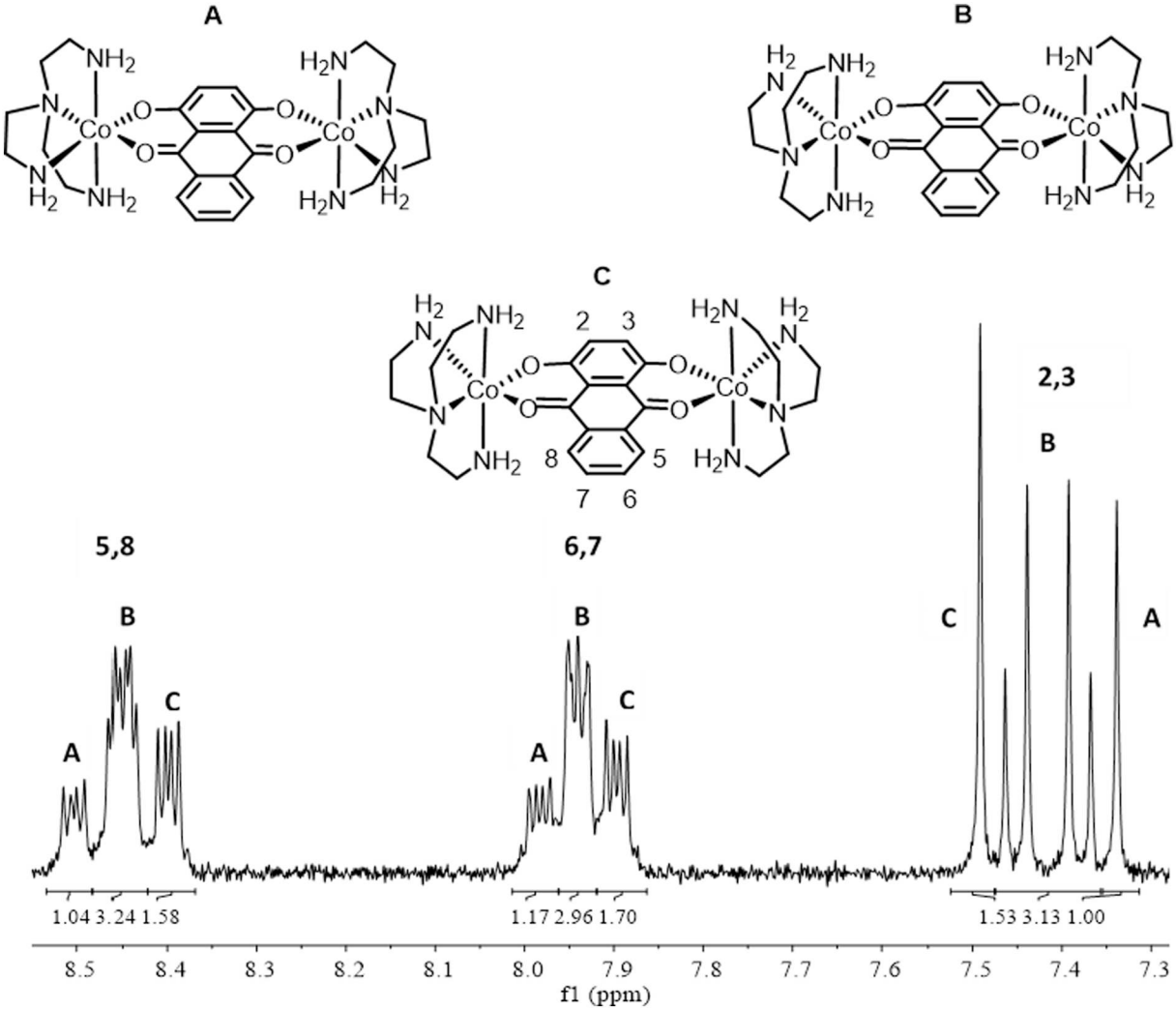

Fig. 2. The aromatic region of the ^{1}H NMR spectrum of $[(Co(tren))_2(quin)](ClO_4)_4$ (**1**) in D_2O. A and C are the supposed structures of the symmetrical isomers while B is the asymmetrical isomer.

2.6. HSA binding studies

2.6.1. Preparation of stock solutions of HSA and the studied complexes and ligands

HSA solution was prepared in phosphate buffered saline (PBS) strictly on the same day when the experiment was performed. Ligand $quinSH_3$ and all complexes were dissolved in PBS buffer at *c.a.* 100 μM concentration. Ligand stock solution of $quinH_2$ was prepared in DMSO (100 μM). Ligand stock solutions were kept in dark and were used within 48 h.

2.6.2. UV–Vis spectrophotometric measurements on HSA binding of the compounds

Two-chamber cuvettes (tandem cells) were utilized to monitor the interaction between HSA and compounds $quinSH_3$, **1** and **4** in PBS puffer. One chamber contained 60 μM compound and the other contained 4–120 μM HSA. Spectra were recorded before and after mixing of the content of the cuvette on an Agilent Cary 8454 diode array spectrophotometer in the wavelength range between 190 and 1100 nm.

2.6.3. Spectrofluorometric measurements

PBS puffer was used for sample preparation; and emission spectra were recorded after 30 min incubation. Three kinds of experiments were carried out: (i) 1 μM HSA and various amounts of compound (from 0 to 15 eq.) were used for quenching experiments; and (ii) fluorescence of site markers WF and DG was examined in samples containing 1 μM HSA, 1 μM marker and 0–15 μM compound; while (iii) intrinsic fluorescence of the ligands was followed as well applying 1 or 0.5 μM ligand and various HSA concentrations (0–15 μM). The excitation and emission wavelengths and applied slit widths are listed in Table S1. Computer program PSEQUAD was utilized for calculation of formation constants for HSA – compound adducts as described in our former work [34].

Corrections for self-absorbance and inner filter effect were done as described in our former work using the formula suggested by Lakowicz [35,36].

Model calculations on the binding stoichiometry of $quinSH_3$ – HSA interaction were carried out for models assuming one (I), two (II) or three (III) available binding sites on the protein. The two binding constants determined in site marker displacement experiments were used for model II; model I operates with log*K*' = 6.30 (average value of the two determined constants), while model III contains the two experimental constant and the average of them assumed for a third site. Calculations were done with MEDUSA program [37].

3. Results and discussion

3.1. Synthesis and characterization

$QuinH_2$ or $quinSH_3$ and stoichiometric amount of $[Co(4\ N)Cl_2]Cl$ (4 N = tren or tpa) precursors were reacted in isopropanol for **1**, **2**,

methanol for **3** and water for **4** in the presence of two eq. base at high temperature (60–70 °C) for 4 h or overnight. Purple crystalline solid appeared on cooling at 4 °C by adding bulky ClO_4^- or PF_6^- anions to the reaction mixture. The novel complexes are air stable, soluble in water in relatively low (0.7–1.0 mM) concentration and stable in aqueous solution at least for 48 h.

The free ligand $quinH_2$ was examined by ^1H NMR in d^6-DMSO. The hydroxyl groups appear as one singulet at 12.7 ppm. Resonances of protons *2* and *3* (see Fig. 1. for the numbering scheme) at 8.25 ppm, *4* and *5* at 7.99 ppm as multiplets and *6*, *7* at 7.44 ppm as a singulet in the spectrum. All of the similar type of protons showed one single peak each in the spectrum, proving the symmetry of the ligand. By adding base to the sample all signals of the aromatic protons showed downfield shift due to deprotonation of the hydroxyl groups. The extent of the shift was 0.29 ppm in the case of protons *2*, *3*, 0.15 ppm for *5*, *8* and nearly 0 ppm (0.01 ppm) for *6*, *7* due to these latter hydrogens are too far from the hydroxyl groups.

The signals of the quinizarin as well as the aliphatic tren protons in the spectra of **1** and **3** complexes are separated well resulting a simple assignation. For illustration ^1H NMR spectrum of **1** is shown in Fig. S1. Comparing the integrals of the resonances of the *6*, *7* protons of quinizarin (around 7.95 ppm) and one of the well separated set of signals of one CH_2 function (around 3.55 ppm) of the tren ligand for instance, the integration values clearly reveal the dinuclear nature of the complexes formed with both of the ligands. In particular, in Fig. 2. the aromatic region of **1** indicates that the *5*, *8* protons of the coordinated ligand exhibit resonances at low field due the neighbouring high electronegativity O donors while the *6*, *7* protons of the same ring show signals at higher field being further apart from these donors. The remaining two *2*, *3* protons of the quinizarin backbone can be found around 7.4 ppm. Looking at the above signals of the protons of the quinizarin backbone in each case three sets of them can be seen. For the *2*, *3* protons instead of the expected three singulets, however, two singulets and a multiplet are detected. These findings indicate that in **1** two symmetrical and one asymmetrical isomers should be present. (This is also clearly demonstrated by the COSY spectrum shown in Fig. S2.) This assumption is further supported by comparing the ratio of integrals of the three isomers for *5*, *8* and *6*, *7* protons. The structure of the expected three isomers can also be seen in Fig. 2. As in isomer B the two Co cores coordinate asymmetrically to the quinizarin the multiplet for the *2*, *3* protons at 7.4 ppm belongs to this isomer and, according to the integrals, this is the major one among the isomers.

Assignation was more difficult for the tpa complexes (**2** and **4**) due to the aromatic character of the three pyridyl arms of the tpa ligand. The -CH_2 groups of tpa appear in the range of 6.00–5.00 ppm. The ratio of the aromatic and aliphatic hydrogens clearly indicates the formation of the same type of dinuclear complexes like in case of the tren analogues. Based on the ^1H NMR spectra of **2** and **4** (not shown) the large number of signals in the well separated –CH_2 region indicate the presence of various isomers.

In order to further elucidate the structure of the complexes ESI-MS analysis in the positive mode was also carried out. In most of the cases in the mass spectra of the products peaks belonging to both mono and dinuclear complexes appeared. Based on the results, Co(III) was reduced to Co(II) in all of the four novel compounds under ESI-MS conditions. Peaks of precursor ions like $[Co(II)(tren)(ClO_4)]^+$ or $[Co(II)(tpa)]^{2+}$ appeared in the spectra in most cases. While in the spectra of quin complexes only the signals of ions containing Co(II) were detected, for the quinS analogues molecule ions containing Co(III) can also be identified. Interestingly, in the spectrum of **4** the m/z = 507.573 value belongs to the $[(Co(III)(tpa))(quinS)(Co(II)(tpa))]^{2+}$ with different oxidation state of the two metal ions. All of the mass spectra displayed the correct isotopic pattern; as a representative example, see Fig. S3.

The identity of the complexes was further proved by the elemental analysis data. It was found for the quinS complexes that the sulfonic acid group is deprotonated in both complexes, thus three counter ions (PF_6^- for **3** and ClO_4^- for **4**) were required for crystallization. The results indicate that complexes **1**, **2** and **4** also contain water molecules in their structures. (Despite all our efforts **1** contains some $NaClO_4$ impurity but this did not affect the results of the CV measurements or HSA binding studies.)

The carbonyl functional groups of the novel complexes involved in the coordination were also studied by IR spectroscopy. The change of the absorption band, assigned to υ(C=O) in all of the novel compounds compared to that of the free ligand $quinH_3$ was observed. The corresponding band at 1630 cm^{-1} in the spectrum of $quinH_3$ has been shifted to the region of 1540–1548 cm^{-1} upon bonding for all four complexes [38,39]. The shift of this band due to complexation with other type of metal ion was reported before [40]. These results confirmed that the ligands are bound to the cobalt ions via the oxygens of the carbonyl groups.

3.2. Electrochemical studies

In order to examine the electrochemical properties of the novel complexes cyclic voltammetric measurements were carried out in the 0 – (−1000) mV voltage range. Since some previous results demonstrated redox activity of the studied ligands, $quinH_2$ and $quinSH_3$, in this voltage range [9,41] prior to the investigation of the metal complexes, measurements on the free ligands in aqueous solution were also performed. In agreement with previous literature findings [9,41] both ligands showed redox activity. For illustration, representative voltammograms are seen in Fig. S4. The voltammograms revealed reversible reduction steps in the range (−450)–(−800) mV vs. Ag/AgCl reference electrode for both of the ligands, but significant differences were also observed when the results for $quinSH_3$ and $quinH_2$ were compared. Namely, the anodic and cathodic peak potential values of $quinSH_3$ were shifted to the less negative voltage region by approximately 150 mV compared to the non-sulfonated ligand $quinH_2$, due to the electron withdrawing character of the sulfonate moiety. As it is shown in Fig. S4, two successive (overlapping) reduction processes were indicated by the voltammogram of $quinSH_3$ while only one is seen in the case of $quinH_2$. However, evaluation of the cathodic peak shows the uptake of two electrons also in this latter case, using the formula published by Guin et al. [42]. These above discussed differences of the redox character of the two ligands were also reported by Guin et al. [9,42].

Although, neutral pH is relevant in biological aspect, to get further information of the redox character of the ligands, in another experiment, pH dependence was also studied. Because of solubility reasons, $quinSH_3$ ligand was selected for these investigations. The measurements were carried out in methanol, using $[NBu_4][BF_4]$ as supporting electrolyte (see details in the Experimental part). Selected voltammograms, together with the peak potential values are shown in Fig. S5. Compared to the nearly neutral condition, the voltammograms changed significantly under acidic conditions (pH ~ 2), but only slightly by adjusting the pH up to ~ 11.5. (Fig. S5). The reversible successive reduction steps appear separately at neutral and basic pH, but turn into one overlapped reversible peak shifted to the less negative potential region in acidic solution. This tendency is in a good agreement with the few literature findings [9,43].

Cyclic voltammetric results on the $[Co(tren)Cl_2]Cl$ and $[Co(tpa)Cl_2]Cl$ precursor complexes were previously reported by us and indicated both compounds to show irreversible reduction, but the peak potential value of the tpa precursor complex was significantly less negative than that of the tren analogue [44].

Electrochemical behaviour of the four novel ternary complexes were characterized as well, representative voltammograms recorded in water (pH ~5) are presented in Fig. 3a and b.

pH-dependence of the redox behaviour was also studied. Selected CV curves and peak potential values are shown in Fig. S6 and Table S2, respectively. The results revealed similar pH-dependence for the ternary complex, $[(Co(tren))_2(quinS)](PF_6)_3$ (**3**) as those of the $quinSH_3$

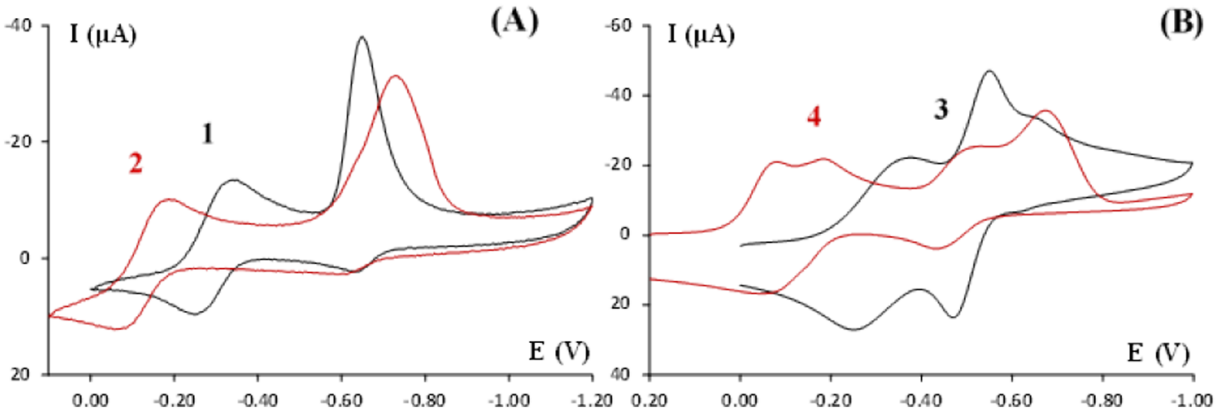

Fig. 3. CV curves registered for $[(Co(tren))_2(quin)](ClO_4)_4$ (**1**), $[(Co(tpa))_2(quin)](ClO_4)_4$ (**2**), $[(Co(tren))_2(quinS)](PF_6)_3$ (**3**) and $[(Co(tpa))_2(quinS)](ClO_4)_3$ (**4**) in water (pH ~5), referenced to Ag/AgCl electrode at a potential sweep rate of 200 mV/s and $c_{complex}$ = 1.0 mM.

ligand.

A comparison between the voltammograms of the free ligands and the corresponding ternary complexes, as well as between those registered for the tren-containing and tpa-containing complexes in Fig. 3a and b shows one significant difference. Namely, one extra reversible process in each of the latter systems compared to the corresponding free ligand is indicated in the voltammograms in the potential range (−400) – 0 mV. All the successive reduction steps are more separated for **4,** while appears as one overlapping peak for the other complexes. The measured cathodic peak potential values of the novel complexes are summarized in Table 1.

The registered extra peaks indicating reversible redox processes in the voltammograms most probably belong to the non-dissociated ternary complex species since none of the possible dissociation products ($quinH_2$/$quinSH_2^-$, $[Co(tren)Cl_2]^+$ (E_{pc} = −439 mV) or $[Co(tpa)Cl_2]^+$ (E_{pc} = 72 mV)) displays similar pattern [42]. Similar observations have been made for the relevant ruthenium containing complexes [28].

In accordance with earlier reports on [Co(4 N)(O,O)] (4 N = tren or tpa, O,O = hydroxamato or quinolonato) type complexes, [44,45] the reduction potentials of tren complexes are more negative than those of the corresponding tpa containing ones. This difference originates from the distinct characters of the N donor atoms of the tripodal amines. While only σ-bonding is possible with the aliphatic N atoms of tren, π-back-bonding interaction occurs with the aromatic pyridyl N donor atoms of tpa. Thus a decreased electron density at the cobalt ions in the complexes of tpa results in species more susceptible for reduction compared to the corresponding tren analogues. Regarding the appropriate quinizarin Co(III) ternary complexes with a given 4 N donor (tren or tpa) auxiliary ligand and (O,O) coordination of the quinizarin the obtained cathodic peak potential values are in the same range as those obtained for the previously studied hydroxamato or quinolonato complexes with identical (O,O) coordination [44,45].

Table 1
Cathodic peak potential values of the novel ternary complexes in water (pH~5), referenced to Ag/AgCl electrode at a potential sweep rate of 200 mV/s and $c_{complex}$ = 1.0 mM.

Complex	E_{pc} (mV) vs. Ag/AgCl
$[(Co(tren))_2(quin)](ClO_4)_4$ (**1**)	−340
	−649
$[(Co(tpa))_2(quin)](ClO_4)_4$ (**2**)	−182
	−734
$[(Co(tren))_2(quinS)](PF_6)_3$ (**3**)	−368
	−553
	−658
$[(Co(tpa))_2(quinS)](ClO_4)_3$ (**4**)	−78
	−193
	−506
	−677

3.3. Lipophilicity measurements

Lipophilicity of the studied ligands and their complexes has not reported in the literature yet. The extremities in the lipophilic and hydrophilic character of $quinH_2$ and the sulfonated complexes required modified experimental conditions, namely the water-to-octanol volume ratio was changed from 1:1 in favor of the less efficient solvent phase (see details in the Experimental part). Table 2 comprises the logarithm of distribution coefficients ($\log D_{7.40}$) determined at pH 7.40.

Ligand $quinH_2$ appears to be highly lipophilic, while its sulfonated congener $quinSH_3$ is significantly hydrophilic thanks to the deprotonated sulfonate functional group on the molecule. Complexes **1** and **2** show similar and remarkable hydrophilic character that can be due to the +4 positive charge of the complex cations. For complexes **3** and **4** only a threshold limit ($\log D_{7.40}$ < −3.0) could be estimated. The extreme hydrophilicity of these sulfonate complexes however is not surprising, considering the *c.a.* 3.5 orders of magnitude difference in $D_{7.40}$ values obtained for $quinH_2$ and $quinSH_3$.

The result of lipophilicity measurements points out the possible cell uptake of the active ligand $quinH_2$ via passive transport, while its complexes require most probably an alternative pathway to enter cells.

3.4. Albumin binding of the ligands and their complexes

HSA is the most abundant transport protein in human blood, providing three hydrophobic binding pockets (site I, II and III) for various types of molecules. Albumin binding may not only increase the apparent solubility of a compound but can prevent its early metabolism and excretion. HSA binding of the compounds was investigated by means of UV–Vis and direct and indirect spectrofluorometric techniques at 37 °C. Limited aqueous solubility of $quinH_2$ allowed the

Table 2
Distribution coefficients ($D_{7.4}$) determined for ligands $quinH_2$ and $quinSH_3$ and their Co(III)-complexes (**1**–**4**), at pH = 7.40 (PBS buffer), 25 °C.

	$\log D_{7.40}$
$quinH_2$	2.95(3)
$quinSH_3$	−0.55(2)
1	−1.33(2)
2	−1.08(2)
3	< −3.0
4	< −3.0

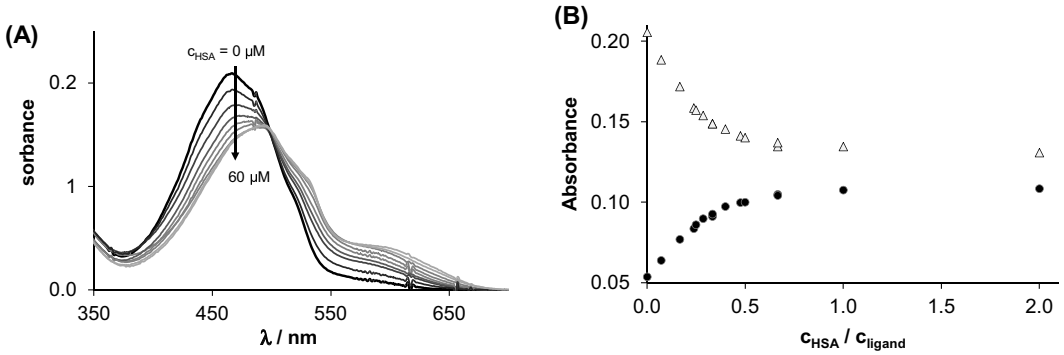

Fig. 4. UV–Vis absorbance spectra recorded for quinSH$_3$ in the absence and presence of HSA in various concentrations (A), and absorbance values followed at 460 nm (Δ) and 530 nm (●) in this system, c_{lig} = 30 μM, pH = 7.40 (PBS), 37 °C.

implementation of only certain fluorometric measurements.

Global binding of quinSH$_3$, **1** and **4** on HSA was investigated by UV–Vis spectrophotometry. Fig. 4 shows the spectral changes of quinSH$_3$ in the presence of increasing HSA concentration. Absorption maxima are red shifted with an isobestic point at 498 nm, and a new band develops between 550 and 650 nm. Structural rearrangement or even partial deprotonation of the ligand (see Fig. S7 for UV–Vis spectrum of the completely deprotonated ligand) is probable upon binding to albumin. The binding takes place fairly fast (within some seconds the equilibrium was reached) and seems to be completed upon the addition of < 1 eq. HSA, that strongly suggests the presence of at least two binding sites for quinSH$_3$ in HSA. On the other hand, complexes **1** and **4** do not show appreciable spectral changes in the presence of the protein even after 2 h waiting time (see Fig. S8). This phenomenon however does not exclude binding of the complexes in HSA, since this event covers more frequently intermolecular, non-covalent interactions that have little (or not measurable) effect on the UV–Vis spectra of a small molecule.

As next step binding at site I (IIA subdomain) was studied via tryptophan (Trp) quenching experiments in the case of quinSH$_3$, **1**, **2**, **3** and **4**. The only Trp (Trp214) in HSA is situated near to site I and can selectively be excited at λ = 295 nm. As Fig. 5 shows Trp exerts strong fluorescence around 340 nm that can be quenched by a binding event at or close to site I [46–48]. Quenching curves in Fig. 5 suggest considerable binding of quinSH$_3$ at this site, while complexes **1**–**4** could not quench the fluorescence of Trp, and consequently may not bind here. Solubility problems of quinH$_2$ hindered the execution of quenching and marker displacement measurements with this ligand. A conditional binding constant logK'_{quench} = 5.92(1) can be computed by the program PSEQUAD for the quinSH$_3$ − site I interaction [34]. Binding affinity of quinSH$_3$ at site I was determined by WF displacement experiments as well. Here competition of the two compounds for site I was revealed again and a similar binding constant (logK' = 6.14(1)) could be calculated. Complexes **1**–**4**, at the same time, do not compete with WF for site I, which is in accordance with the findings of quenching experiments.

Site marker DG was utilized to follow binding at the other main binding pocket site II (IIIA subdomain). High extent of quinSH$_3$ binds to site II; the calculated affinity logK' = 6.45 (2) exceeds reported binding strength of diazepam that is a well-known high-affinity ligand of site II (log$K$ = 5.6) [46]. The metal complexes do not show binding at site II.

The studied ligands quinSH$_3$ and quinH$_2$ possess moderate intrinsic fluorescence favorably not overlapping by that of HSA (see Fig. S9); and effect of the protein on this fluorescence was investigated as well. Samples contained ligands in highly diluted solution (1.0 and 0.5 μM for quinSH$_3$ and quinH$_2$ respectively) and various equivalents of HSA, which allowed to study the HSA binding of quinH$_2$ itself. Fig. 6a shows the intensity changes of quinSH$_3$ in the presence of the protein and an unequivocal decrease in the intensity can be observed. Albumin binding, providing a solvent protected non-polar environment often enhances fluorescence of a small-molecule. UV–Vis experiments however, formerly suggested structural changes, even partial deprotonation of quinSH$_3$ upon binding to HSA. Besides, fluorescence measurements reveal negligible fluorescence of the deprotonated form of quinSH$_3$ (Fig. S9). Namely, assisted deprotonation of quinSH$_3$ upon binding to HSA is a possible explanation of the unusual fluorescence quenching effect of the protein on the ligand's intrinsic fluorescence.

Model calculations were performed with the help of binding constants determined for sites I and II in order to get an insight into the binding stoichiometry between HSA and this ligand. In Fig. 6 the two-site model (assuming binding at both sites I and II) gives the best fit to the experimental data, while one-site or three-site models deviate considerably from those. In all, high affinity binding of two equivalents of quinSH$_3$ is probable on HSA, but existence of a low-affinity (log$K$ < 5) third site cannot be excluded. The emission intensity of quinH$_2$ is quenched as well upon addition of HSA (see Fig. 6), however

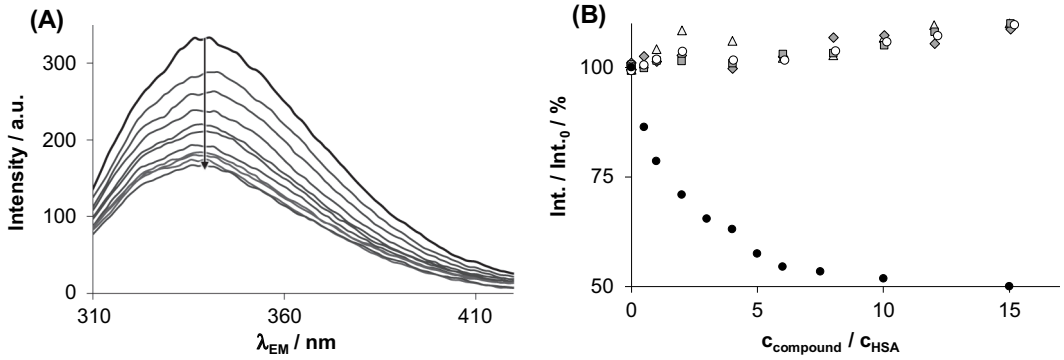

Fig. 5. Trp214 fluorescence spectra of HSA in the presence of increasing quinSH$_3$ concentrations (0–15 μM) (A) and normalized fluorescence quenching curves registered at $λ_{EM}$ = 350 nm for quinSH$_3$ (●), **1** (◊), **2** (□), **3** (Δ) and **4** (○) at various compound-to-HSA ratios, c_{HSA} = 1 μM; $λ_{EX}$ = 295 nm; pH = 7.40 (PBS), 37 °C.

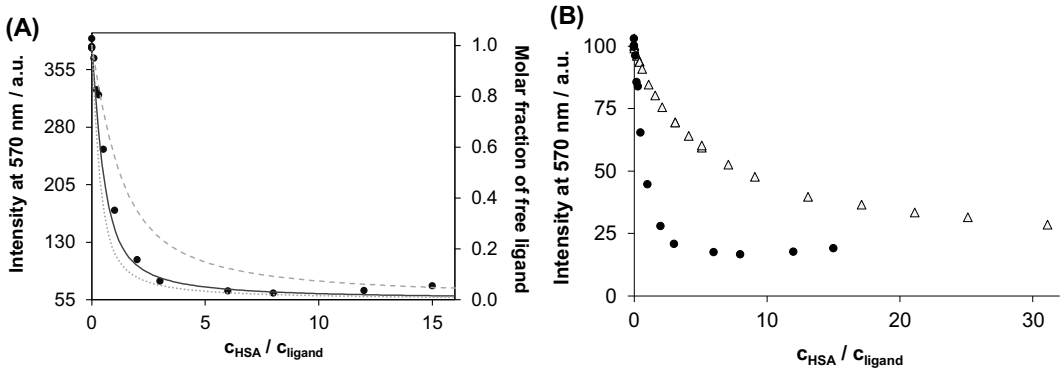

Fig. 6. Intrinsic fluorescence of $quinSH_3$ (●) at various HSA concentrations monitored at λ_{EM} = 570 nm and calculated molar fractions of the non-bound ligand for hypothesized one- (dashed curve), two- (solid curve) or three- (dotted curve) binding sites in HSA (A). Comparison of the fluorescence quenching curves of $quinSH_3$ (●) and $quinH_2$ (Δ) upon addition of HSA (B), c_{lig} = 1 μM ($quinSH_3$) or 0.5 μM ($quinH_2$), λ_{EX} = 480 nm; pH = 7.40 (PBS), 37 °C. Binding constants used for the model calculations: $logK'_{site-1}$ = 6.14, $logK'_{site-2}$ = 6.45, $logK'_{site-3}$ = 6.30.

its protracted quenching curve assumes considerably lower affinity and/or less accessible binding sites for $quinH_2$ compared to that of $quinSH_3$.

All in all, both ligands bind to HSA, however in different manner. $QuinSH_3$ has two high affinity binding sites (at sites I and II) on albumin, while $quinH_2$ shows lower affinity towards the protein. The different affinity of the two types of ligands can be interpreted by the negative charge (− and/or 2−) of $quinSH_3$ at pH 7.4 that may contribute to the stronger binding on HSA of this ligand over the neutral $quinH_2$. The appropriate Co(III)-complexes of the two ligands do not seem to bind to HSA.

4. Conclusions

Based on their thermodynamic stability, kinetic inertness and redox features the synthesized quinizarin-containing ternary cobalt(III) complexes may serve as models for anthracycline type drug chaperons being able to selectively release the drug molecules in hypoxic cancer tissues. Structural characterization of the complexes supports the formation of dinuclear species being present in various binding isomers. For **1** the presence of two symmetrical and one asymmetrical isomer was confimed by detailed NMR studies. Cyclic voltammetric results indicate redox activity of the ligands $quinH_2$ and $quinSH_3$. At the same time for the Co(III) complexes further reversible processes were detected. Reversible reduction for the tren containing complexes occurs in the potential range of biological relevance (−200 to −400 mV). HSA binding studies of the free ligands as well as the Co(III) complexes revealed that $quinSH_3$ interacts with hydrophobic pockets site I and II of the protein, while for $quinH_2$ a significantly lower affinity towards the protein was demonstrated. On the contrary, complexes **1–4** did not exhibit significant binding to HSA. Based on the reduction potential values the studied complexes may selectively be reduced under hypoxic conditions and both the quin (or anthracycline) ligands and the Co(II) formed, by initiating ROS formation, can exert they biological effect. Currently further biological studies are in progress with the novel ternary complexes to obtain further information on their in vitro efficacy.

Declaration of competing interest

The authors declare no conflict of interest.

Acknowledgement

The research was supported by the EU and co-financed by the European Regional Development Fund under the projects GINOP-2.3.2-15-2016-00008, GINOP-2.3.2-15-2016-00038 and the Hungarian Scientific Research Fund (OTKA K112317, FK 124240) and the ÚNKP-19-3-I-DE-45, ÚNKP-19-3-I-DE-56 New National Excellence Program of the Ministry for Innovation and Technology.

Appendix A. Supplementary data

Supplementary data to this article can be found online at https://doi.org/10.1016/j.jinorgbio.2019.110963.

References

[1] D. Agudelo, P. Bourassa, G. Bérubé, H.A. Tajmir-Riahi, J. Photochem. Photobiol. 158 (2016) 274–279.
[2] P. Ma, R.J. Mumper, J. Nano Today 8 (2013) 313–331.
[3] C. Carvalho, R.X. Santos, S. Cardoso, S. Correia, P.J. Oliveira, M.S. Santos, P.I. Moreia, Curr. Med. Chem. 16 (2009) 3267–3285.
[4] G. Minotti, P. Menna, E. Salvatorelli, G. Cairo, L. Gianni, Pharmacol. Rev. 56 (2004) 185–229.
[5] S. Goto, Y. Ihara, Y. Urata, S. Izumi, K. Abe, K. Toji, T. Kondo, FASEB J. 15 (2001) 2702–2713.
[6] F. Yao, J. Duan, Y. Wang, Y. Zhang, Y. Guo, H. Guo, X. Kang, Anal. Chem. 87 (2015) 338–342.
[7] D. Agudelo, P. Bourassa, M. Beauregard, G. Bérubé, H.A. Tajmir-Riahi, PLoS One 8 (2013) 1–8 (e69248).
[8] S. Zhang, X. Liu, T. Bawa-Khalfe, L.S. Lu, Y.L. Lyu, L.F. Liu, E.T. Yeh, Nat. Med. 18 (2012) 1639–1642.
[9] P.S. Guin, S. Das, P.C. Mandal, Int. J. Electrochem. Sci. 3 (2008) 1016–1028.
[10] H. Muhammed, T. Ramasarma, C.K.R. Kurup, Biochim. Biophys. Acta 722 (1982) 43–50.
[11] E. Goormaghtigh, J.M. Ruysschaert, Biochim. Biophys. Acta 779 (1984) 271–288.
[12] E.J.F. Demant, Eur. J. Biochem. 137 (1983) 113–118.
[13] E.J.F. Demant, P.K. Jensen, Eur. J. Biochem. 132 (1983) 551–556.
[14] Y. Iwamoto, I.L. Hansen, T.H. Porter, K. Folkers, Biochem. Biophys. Res. Commun. 58 (1974) 633–638.
[15] T. Goodman, P. Hoschstein, Biochem. Biophys. Res. Commun. 77 (1977) 797–803.
[16] E. Bachmann, E. Weber, G. Zbinder, Agents Actions 5 (1975) 383–393.
[17] V.J. Ferrans, Cancer Treat. Rep. 62 (1978) 955–961.
[18] K.D. Mjos, J.F. Cawthray, G. Jamieson, J.A. Fox, C. Orvig, Dalton Trans. 44 (2015) 2348–2358.
[19] E. Gammella, F. Maccarinelli, P. Buratti, S. Recalcati, G. Cairo, Front. Pharmacol. 5 (2014).
[20] Y. Octavia, G.C. Tochetti, L.K. Gabrielson, S. Janssens, J.H. Crijns, L.A. Moens, J. Mol. Cell. Cardiol. 52 (2012) 1213–1225.
[21] M. Sterba, O. Popelova, A. Vavrova, E. Jirkovsky, P. Kovarikova, V. Gersl, Antioxid. Redox Signal. 18 (2013) 899–929.
[22] H. Beraldo, A. Garnier-Suillerot, L. Tosi, F. Lavelle, Biochemistry 24 (1985) 284–289.
[23] M.M.L. Fiallo, A. Garnier-Suillerot, Biochemistry 25 (1986) 924–930.
[24] M.M.L. Fiallo, A. Garnier-Suillerot, Biochim. Biophys. Acta (Gen. Subject) 840 (1985) 91–98.
[25] M. Feng, Y. Yang, P. He, Y. Fang, Spectrochim. Acta A 56 (2000) 581–587.
[26] P.S. Guin, P.C. Mandal, S. Das, J. Coord. Chem. 65 (2012) 705–721.
[27] S. Maji, B. Sarkar, S.M. Mobin, J. Fiedler, F.A. Urbanos, R. Jimenez-Aparicio, W. Kaim, G.K. Lahiri, Inorg. Chem. 47 (2008) 5204–5211.
[28] A. Mandal, A. Grupp, B. Schwederski, W. Kaim, G.K. Lahiri, Inorg. Chem. 54 (2015) 7936–7944.
[29] D.C. Ware, B.D. Palmer, W.R. Wilson, W.A. Denny, J. Med. Chem. 36 (1993) 1839–1846.

[30] J. Jiang, C. Auchinvole, K. Fischer, C.J. Cambell, Nanoscale 6 (2014) 12104–12110.
[31] Z. Tyeklár, R.R. Jacobson, N. Wei, N.N. Murthy, J. Zubieta, K.D. Karlin, J. Am. Chem. Soc. 115 (1993) 2611–2689.
[32] E. Kimura, S. Young, J.P. Collman, Inorg. Chem. 9 (1970) 1183–1191.
[33] E. Farkas, P. Buglyó, É. Enyedy, M.A. Santos, Inorg. Chim. Acta 357 (2004) 2451–2461.
[34] L. Zékány, I. Nagypál, Plenum Press, (1985) 291–353.
[35] O. Dömötör, S. Aicher, M. Schmidlehner, M.S. Novak, A. Roller, M.A. Jakupec, W. Kandioller, C.G. Hartinger, B.K. Keppler, É.A. Enyedy, J. Inorg. Biochem. 134 (2014) 57–65.
[36] J.R. Lakowicz, Principles of Fluorescence Spectroscopy, 3rd ed., Springer, 2006.
[37] Make Equilibrium Diagrams Using Sophisticated Algorithms, https://www.kth.se/che/medusa, Accessed on 24 September 2019.
[38] G. Smulevich, L. Angeloni, S. Giovannardi, M.P. Marzocchi, Chem. Phys. 65 (1982) 313–322.
[39] X. Xuan, X. Wang, N. Wang, Spectrochim. Acta A 79 (2011) 1091–1098.
[40] M. Shamsipur, A. Besharati-Seidani, React. Funct. Polym. 71 (2011) 131–139.
[41] D. Nematollahi, A. Sayadi, F. Varmaghani, J. Electroanal. Chem. 671 (2012) 44–50.
[42] P.S. Guin, P. Das, S. Das, P.C. Mandal, Int. J. Electrochem. 2012 (2011) 1.
[43] B. Zinger, J. Electroanal. Chem. 239 (1988) 209–225.
[44] P. Buglyó, I. Kacsir, M. Kozsup, I. Nagy, S. Nagy, A.C. Bényei, E. Kováts, E. Farkas, Inorg. Chim. Acta 472 (2018) 234–242.
[45] M. Kozsup, E. Farkas, A.C. Bényei, J. Kasparkova, H. Crlikova, V. Brabec, P. Buglyó, J. Inorg. Biochem. 193 (2019) 94–105.
[46] J. Peters, All About Albumin, Biochemistry, Genetics, and Medical Applications, Academic Press, 1996.
[47] G. Fanali, A. di Masi, V. Trezza, M. Marino, M. Fasano, P. Ascenzi, Mol. Asp. Med. 33 (2012) 209–290.
[48] G. Sudlow, D.J. Birkett, D.N. Wade, Mol. Pharmacol. 12 (1976) 1052–1061.